SAND2023-01517

SANDIA REPORT

SAND2023-01517
Printed April 2023

Sandia National Laboratories

Acoustic Research under the Source Physics Experiment

Trevor W. Wilson
Geophysical Detection Programs
Sandia National Laboratories
P.O. Box 5800
Albuquerque, NM 87185-9999
tcwils@sandia.gov

Philip S. Blom
Earth and Environmental Sciences
Los Alamos National Laboratory
Los Alamos, NM 87544
pblom@lanl.gov

Fransiska K. Dannemann Dugick
Geophysical Detection Programs
Sandia National Laboratories
P.O. Box 5800
Albuquerque, NM 87185-9999
fkdanne@sandia.gov

Daniel C. Bowman
Geophysical Detection Programs
Sandia National Laboratories
P.O. Box 5800
Albuquerque, NM 87185-9999
dcbowma@sandia.gov

Keehoon Kim
Department of Earth Sciences
Lawrence Livermore National Laboratory
Livermore, CA 94550
kim84@llnl.gov

Prepared by
Sandia National Laboratories
Albuquerque, New Mexico 87185
Livermore, California 94550

Sandia National Laboratories
U.S. DEPARTMENT OF ENERGY NNSA

Sandia National Laboratories is a multimission laboratory managed and operated by National Technology & Engineering Solutions of Sandia, LLC, a wholly owned subsidiary of Honeywell International Inc., for the U.S. Department of Energy's National Nuclear Security Administration under contract DE-NA0003525.

Issued by Sandia National Laboratories, operated for the United States Department of Energy by National Technology & Engineering Solutions of Sandia, LLC.

Available to DOE and DOE contractors from

U.S. Department of Energy
Office of Scientific and Technical Information
P.O. Box 62
Oak Ridge, TN 37831

Telephone: (865) 576-8401
Facsimile: (865) 576-5728
E-Mail: reports@osti.gov
Online ordering: http://www.osti.gov/scitech

Available to the public from

U.S. Department of Commerce
National Technical Information Service
5301 Shawnee Road
Alexandria, VA 22312

Telephone: (800) 553-6847
Facsimile: (703) 605-6900
E-Mail: orders@ntis.gov
Online order: https://classic.ntis.gov/help/order-methods

Acoustic Research under the Source Physics Experiment

Trevor W. Wilson
Geophysical Detection Programs
Sandia National Laboratories
P.O. Box 5800
Albuquerque, NM 87185-9999
tcwils@sandia.gov

Fransiska K. Dannemann Dugick
Geophysical Detection Programs
Sandia National Laboratories
P.O. Box 5800
Albuquerque, NM 87185-9999
fkdanne@sandia.gov

Daniel C. Bowman
Geophysical Detection Programs
Sandia National Laboratories
P.O. Box 5800
Albuquerque, NM 87185-9999
dcbowma@sandia.gov

Keehoon Kim
Department of Earth Sciences
Lawrence Livermore National Laboratory
Livermore, CA 94550
kim84@llnl.gov

Philip S. Blom
Earth and Environmental Sciences
Los Alamos National Laboratory
Los Alamos, NM 87544
pblom@lanl.gov

SAND2023-01517

ABSTRACT

The Source Physics Experiment series is a long-term research and development (R&D) effort under the U.S. Department of Energy's National Nuclear Security Administration focused on improving the physical understanding of how chemical explosions generate seismoacoustic signals. Beginning in 2011, a series of subsurface chemical explosions in two different and highly contrasting geologies were conducted at the Nevada National Security Site in Nevada, USA with the objective of improving simulation and modeling approaches to explosion identification, yield estimation and other monitoring applications. The two executed phases of the series provide new explosion signature source data from a wide range of geophysical diagnostic equipment; recorded data from the test series is now openly available to the broader seismoacoustic community. This manuscript details the executed test series, deployed seismoacoustic networks, and summarizes major scientific achievements utilizing recorded signatures from the explosive tests.

Acknowledgment

This paper describes objective technical results and analysis. Any subjective views or opinions that might be expressed in the paper do not necessarily represent the views of the U.S. Department of Energy or the United States Government. Sandia National Laboratories is a multimission laboratory managed and operated by National Technology & Engineering Solutions of Sandia, LLC, a wholly owned subsidiary of Honeywell International Inc., for the U.S. Department of Energy's National Nuclear Security Administration under contract DE-NA0003525. The Source Physics Experiments (SPE) would not have been possible without the support of many people from several organizations. The authors wish to express their gratitude to the National Nuclear Security Administration, Defense Nuclear Nonproliferation Research and Development (DNN R&D), and the SPE working group, a multi-institutional and interdisciplinary group of scientists and engineers.

CONTENTS

LIST OF FIGURES

LIST OF TABLES

0.1. Introduction

The Source Physics Experiment (SPE) series is a long-term research and development (R&D) effort under the U.S. Department of Energy's National Nuclear Security Administration (NNSA) focused on improving U.S capabilities for monitoring. Chemical explosions are used as a surrogate to further improve the physical understanding of how explosions generate seismoacoustic signals as well as developing advanced numerical simulation capabilities from explosive data [Snelson et al., 2013]. The direct application of improved simulation and modeling approaches to explosion identification, yield estimation and other monitoring applications are the principle objective of the test series. To accomplish such, a series of subsurface chemical explosions in two different and highly contrasting geologies, granite (Phase I), and alluvium, (Dry Alluvium Geology (DAG); Phase II), were conducted at the Nevada National Security Site (NNSS) in Nevada, USA. The series is a collaborative effort among Lawrence Livermore National Laboratory (LLNL), Los Alamos National Laboratory (LANL), Sandia National Laboratories (SNL), Mission Support and Test Services, LLC (MSTS) and the Defense Threat Reduction Agency (DTRA). Additional organizations including the University of Nevada, Reno (UNR), the Desert Research Institute (DRI), the Air Force Technical Applications Center (AFTAC) and Silixa, LLC participated in data acquisition and compilation efforts.

The purpose of these tests is to obtain experimental data to aid with discrimination between underground detonations and earthquakes, along with determining methods for utilizing pre-existing world-wide seismic networks for near-real to real time event discrimination [Snelson et al., 2011]. The two executed phases of the series provide new explosion signature source data from a wide range of diagnostic equipment (e.g. seismic, acoustic, electromagnetic surface photogrammetry, etc.) across emplacement conditions lacking such data. Recorded data can be used to update current event characterization semi-empirial methodologies derived from historical test series. Recorded data from the test series is now available to the broader seismoacoustic community via the Incorporated Research Institutions of Seismology (IRIS) as compiled datasets, see [Larotonda and Townsend, 2021, Townsend and Mercadente, 2014, Townsend and Obi, 2015, Townsend and Obi, 2017, Townsend et al., 2019]. This newly publicly available dataset is an asset to the seismoacoustic community as underground sources such as explosions and earthquakes produce acoustic waves in the atmosphere through coupling with seismic energy [Arrowsmith et al., 2010]. Results utilizing the recorded explosions demonstrate that the presence or absence of recorded acoustic energy can aid in constraints on explosion depth of burial and yield estimates [Ford et al., 2014, Bowman, 2019]. Within this summary document we first provide an overview of the executed SPE test series. We detail seismoacoustic networks deployed for each test series and highlight data availability. We provide a summary of prior acoustic work across the SPE/DAG program as a community reference. We highlight how acoustic research under the SPE program has improved our scientific understanding of spall generation mechanisms, rock damage and driven block motions above a buried source of interest. Finally, we evaluate the impacts of the SPE acoustic program against original programmatic science goals.

0.2. Source Physics Experiment (SPE) Overview

0.2.1. Phase I

Phase I of the SPE program was conducted over a 5 year period from 2011 - 2015. The series consists of 6 underground chemical explosions carried out at Climax Stock in northern Yucca Flat at the NNSS. This location is a highly fractured granite body, with well-known characteristics due to the many geological evaluations of the area [Simmons et al., 2003]. The details of each of these detonations: ground truth (GT) time, yield, depth, and scaled depth of burial (SDOB), can be found in Table 0-1.

Shot	Date	Yield (metric tons)	Depth (m)	SDOB ($m/kg^{1/3}$)
SPE-1	2011/05/03 - 22:00:00	0.088	55.1	12.37
SPE-2	2011/10/25 - 19:00:00	0.997	45.7	4.60
SPE-3	2012/07/24 - 18:00:00	0.905	47.3	4.75
SPE-4'	2015/05/21 - 18:36:00	0.089	87.2	19.49
SPE-5	2016/04/26 - 20:49:00	5.035	76.5	4.46
SPE-6	2016/10/12 - 18:36:00	2.245	31.4	2.39

Table 0-1. Details of each of the SPE series detonations

Phase I instrumentation included borehole and surface accelerometers, broadband and short-period seismometers, airplane-mounted synthetic aperture radio, drone photogrammetry, and infrasound microbarometers [Bowman, 2019]. The construction of the SPE-N test bed began in 2010; ground zero (GZ) was a 61 m deep, 91 cm diameter hole. Six instrument holes, each 20 cm in diameter and 58 m deep, were placed in two rings around GZ at horizontal distances of 10 m and 20 m. Each of these boreholes was characterized by performing a multitude of tests including geophysical logs, material property measurements and high-resolution seismic refraction and reflection studies [Snelson et al., 2011]. To characterize the near field of the detonations, each instrument hole had three accelerometers placed at depths of 15, 46, and 55 m. The inner and outer radial instrument holes were offset from each other to optimize azimuthal coverage of measurements. To obtain far-field seismic measurements, geophones and accelerometers were placed around GZ on the surface. While far-field infrasound monitoring included over 32 infrasound sensors placed at distances of 250 m to 5 km from GZ. The locations of the infrasound sensors and accelerometers relative to GZ are shown in Fig.0-1.

Each of the Phase I infrasound arrays shown in Fig. 0-1 consisted of four microbarometers separated by approximately 30 m. For the first two experiments (SPE-1 and SPE-2) the microphones were InterMountain Lab units, which have a flat response between 2 and 30 Hz [Hart, 2007]. Following SPE-2 the InterMountain Lab units were replaced by Hyperion microbarometers. These updated sensors have a much improved flat response between 0.1–100 Hz [Jones et al., 2014]. These Hyperion sensors were used for all remaining SPE tests (3-6). Instruments were outfitted with porous hoses and high frequency wind shrouds for wind noise mitigation. Prior to SPE-5, the four arrays closest to GZ (IS1-IS4) were upgraded to seismically decoupled Hyperions [Bowman, 2019, Townsend et al., 2019].

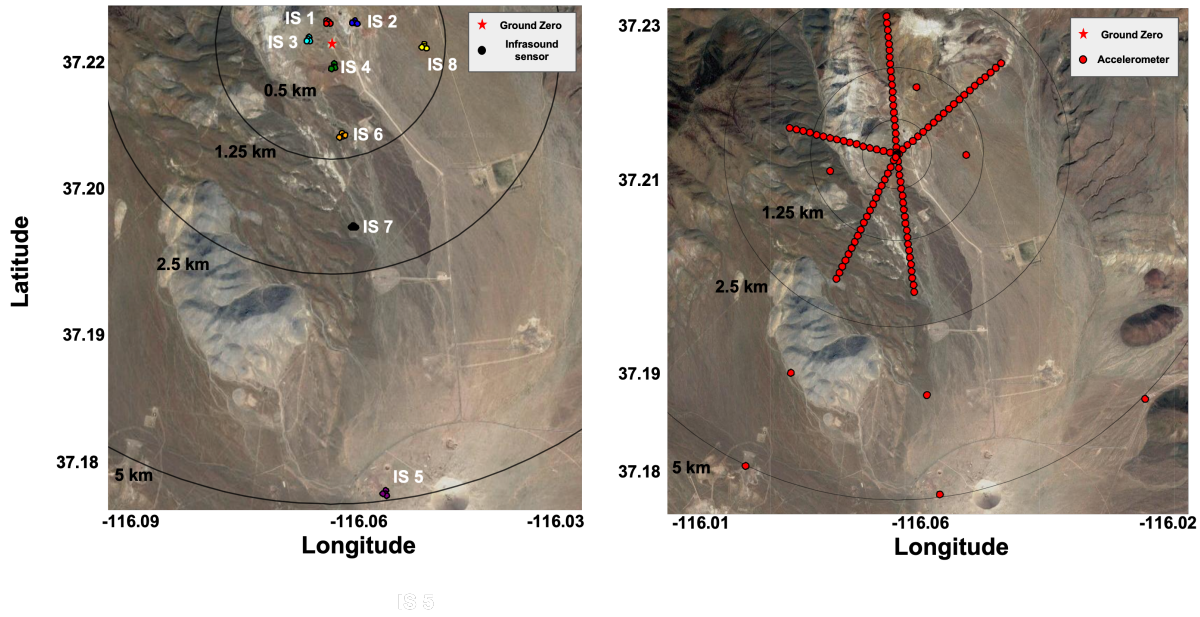

Figure 0-1. Locations for infrasound stations (left) and surface accelerometers near GZ (right) for SPE Phase I. Each infrasound location is an array of microphones.

0.2.2. Phase II: Dry Alluvium Geology

Phase II, Dry Alluvium Geology or DAG, of the program was conducted from 2018 - 2020. This second set of underground chemical explosions consisted of 4 detonations that occurred in alluvium instead of granite. These detonations had depths ranging from 50 to 385 m and yields between 908 and 51000 kg TNT equivalent. The depth of Phase II was much shallower than Phase 1, this was done because alluvium can reduce seismic amplitudes by an order of magnitude compared with granite [Werth and Herbst, 1963]. Yield sizes were also selected to be on the order of 10 times larger than SPE Phase I [Larotonda and Townsend, 2021].

Shot	Date	Yield (metric tons)	Depth (m)	SDOB ($m/kg^{1/3}$)
DAG-1	2018/07/20 - 16:51:52	0.908	385	39.76
DAG-2	2018/12/19 - 18:45:56	50.997	299.8	8.08
DAG-3	2019/04/27 - 15:49:01	0.908	149.9	15.47
DAG-4	2019/06/22 - 21:06:19	10.357	51.6	2.33

Table 0-2. Details of each of the DAG shots.

Many different sensors were deployed during the DAG tests to capture seismoacoustic signals. These sensors were deployed in either the near-field (200 m or less from GZ) or the far-field. Near-field instrumentation included accelerometers deployed on the surface as well in boreholes. These boreholes were drilled at distances of 10, 20, 40, and 80 m from the source hole. A surface accelerometer array was placed within 200 m of GZ with a focus of capturing the spall and supplementing the borehole sensors. The number of surface accelerometers changed between tests: DAG-1 had 24 sensors, DAG-2 and DAG-3 had 42, and DAG-4 had 48. For the far-field, a

collection of geophones, accelerometers and broadband sensors were deployed. The main geophone and accelerometer locations near GZ can be seen in Fig. 0-2. A large geophone array was also deployed near GZ called the "Large N" array, which consisted of 496 closely spaced geophones. To measure the infrasound signals from the tests, several different microbarometer deployments were used. The primary infrasound array (as shown in Fig. 0-2) consisted of 32 Hyperion sensors deployed between 0.5 and 2 km from GZ [Larotonda and Townsend, 2021]. All the sensors located at the range of 0.5 km from the source were seismically decoupled sensors while the non-decoupled sensors were co-located with "null" sensors (insensitive to pressure changes) to help remove non-acoustic signals from the non-decoupled sensors. Additional ground-based acoustic instrumentation included a linear array consisting of 7 Gem infrasound microbarometers, [Anderson et al., 2018] for DAG-1 and an additional microbarometer at GZ for DAG-4.

Infrasound generated by an underground explosion is expected to be highly directional, with most of the acoustic radiation directed upward [Jones et al., 2014, Blom et al., 2020]. It was therefore a goal of the SPE acoustics program to obtain infrasound recordings above the source. This proved to be a logistical challenge. Initial efforts to record signals using infrasound microbarometers carried aloft by octocopters were unsuccessful due to issues with the flight system and instrumentation. Aerial acoustic recording using tethered aerostats and low altitude drifting balloons were likewise unsuccessful, mainly due to the logistics of deployment vs. the timing of the explosions. Aboveground recordings were finally achieved by mounting Gem microbarometers on a nearby crane as well as high altitude balloons.

A single Gem microbarometer was mounted on a crane about 100 m from the borehole and about 30 m above the ground for both DAG-3 and DAG-4. The microbarometer recorded an acoustic signal for both events (Fig. 0-3). The DAG-3 observation is notable because the ground acoustic array did not record infrasound from that event. The origin of the signal recorded on the crane has not been studied in detail, but it may be related to either directional radiation from the epicenter or ground/air coupling of ground motion beneath the crane. The DAG-4 signal shows both an initial phase similar to the one on DAG-3, plus another phase that resembles that recorded on the ground infrasound array.

Gem microbarometers were deployed on solar hot air balloons [Bowman et al., 2020] to record possible directional infrasound from DAG-3 and DAG-4. Strong eastward-blowing winds carried the balloons out of detection range for the DAG-3 event, but one balloon did record infrasound from DAG-4 as reported in [Bowman and Krishnamoorthy, 2021]. They found that this signal was not directional, but rather a nearly horizontally propagating wave that refracted upward into the atmosphere. The balloon-borne detection was achieved at a range of 56 km, while a ground station at about 44 km distance did not capture the signal. The enhanced recording range of the balloon was attributed to lower background noise and the upward-focusing effect of the troposphere. The signal was nearly identical in form to those recorded on the ground and on the crane (Fig. 0-3).

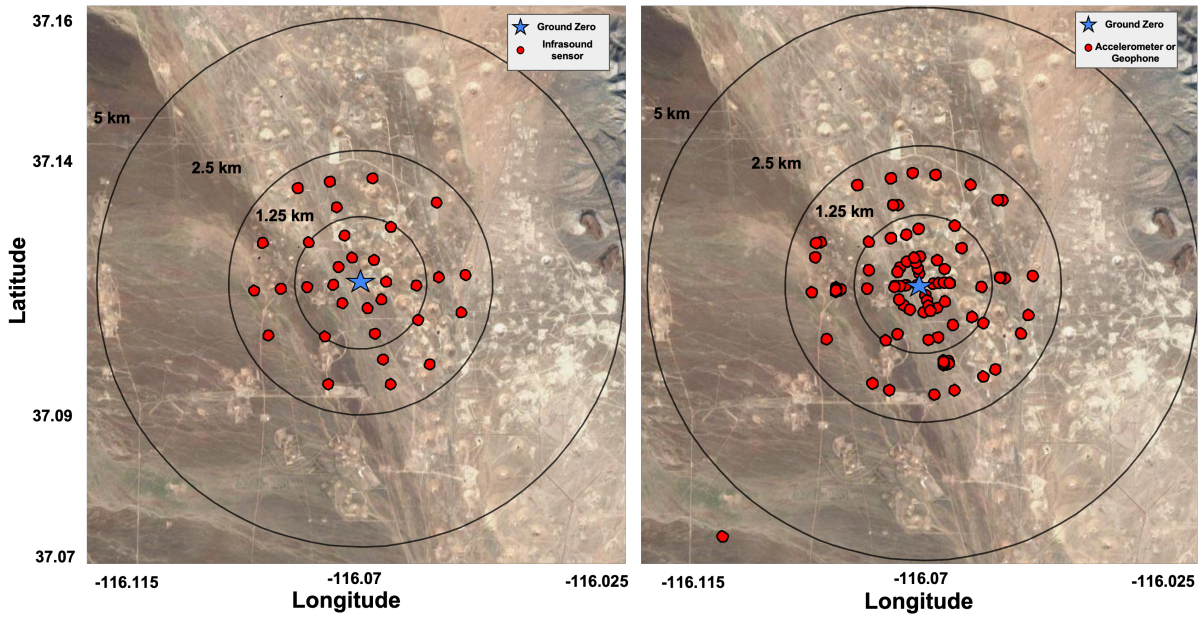

Figure 0-2. Locations for the 32 primary infrasound sensor locations (left) and primary accelerometers (right) for the DAG experiments with respect to GZ .

0.3. Previous Studies of SPE Data

One of the first uses of the SPE acoustic data was in [Jones et al., 2014], where a model was produced for the infrasound generated from the second underground explosion (SPE-2) utilizing the Rayleigh integral to predict far-field propagation. Measurements were made from less than 5 km away, greatly reducing the effects of atmospheric propagation and allowing for a better analysis of the source. To predict the generation mechanism, a model was built based on the analogy of the ground acting as a piston mounted in an infinite baffle. The surface region that moves because of the explosion is modeled as a piston while the surrounding region is the baffle. The attributes that determine the hypothetical area of the piston include the yield, depth, and local geological conditions. Using this model, along with inputs from the surface accelerometers, the Rayleigh integral (RI) was used to generate synthetic infrasound signals. This resulted in similar behavior and shape between the generated and real sets of data as shown in Fig. 0-5. This figure highlights the similarities between synthetic and real signals at all of the infrasound sensors during SPE-2. However, there are small differences between the signals that are hypothesized to be effects of topology, atmospheric conditions, or other assumptions that went into the synthetic model.

[Bowman, 2019] investigates the relationship between the measured acoustic signatures and various source characteristics such as depth and yield (Y). Before analyzing the acoustic data from the SPE experiments, attempts were made to reduce the interference in the signal caused by the local ground motion at the receivers. Due to the proximity of the sensors to GZ, seismic and acoustic signals could overlap. At larger distances this is normally not an issue due to the order of magnitude difference between seismic and acoustic propagation speeds. The first observation made in this study is that the peak acoustic amplitude was best fit by a linear model for yield

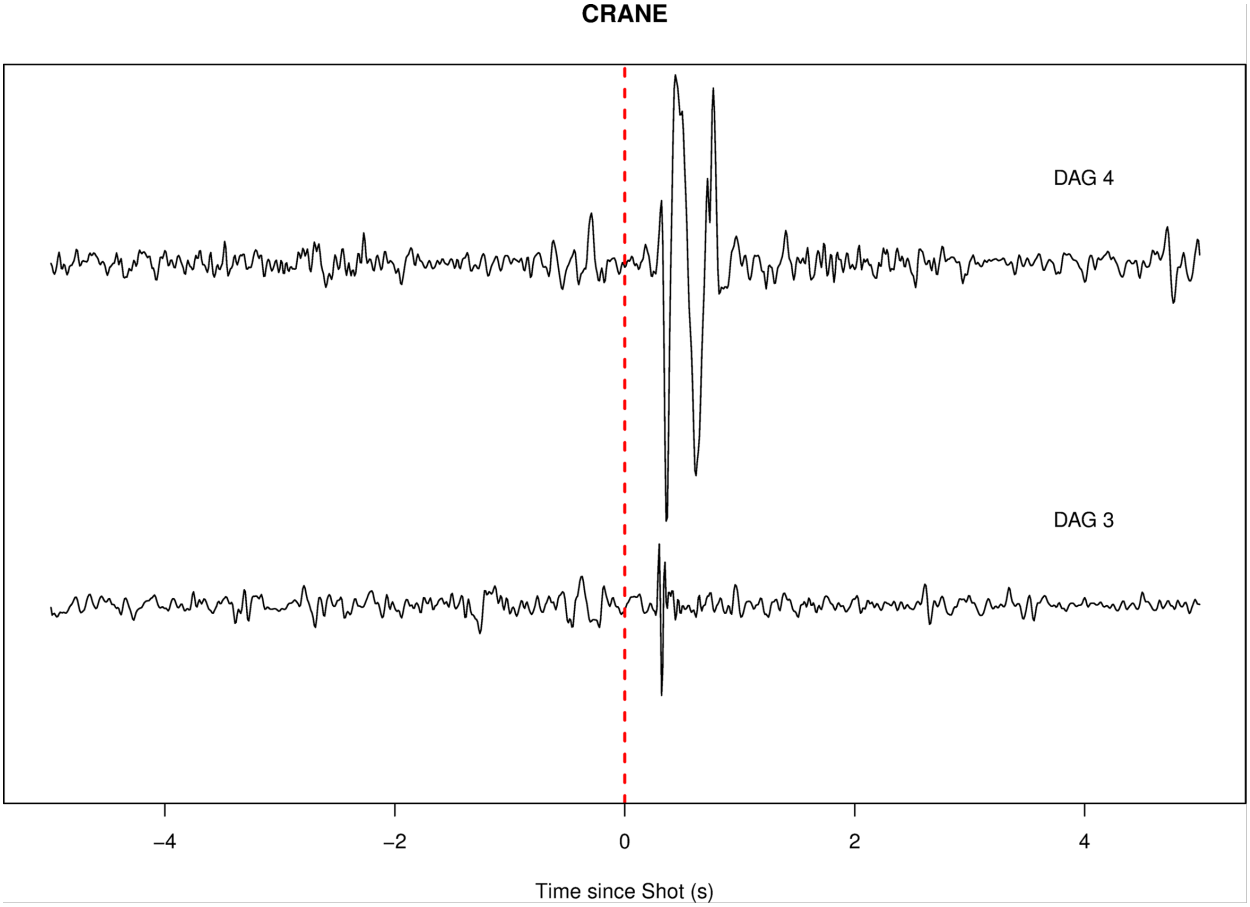

Figure 0-3. Acoustic observations recorded on a Gem microbarometer mounted on a crane near ground zero.

divided by depth. This differs from previous studies of surface and aerial explosions which typically have a a cube root scaling [ANSI, 1983]. The next observation was that cube root of the yield was proportional to the peak frequency, a result consistent with the $Y^{1/3}$ relationship seen in aerial detonations, discussed in [Kinney and Graham, 2013]. This relationship between yield and peak frequency may be driven by effects from spall, an effect of underground explosions where a mass of material enters free fall, impacting competent material below [Bowman et al., 2014]. [Patton, 1990] suggests that the radial extent of spall can be scaled as $Y^{0.26\pm0.03}$. This suggestion fits well with the results of the SPE events; SPE-4' is an outlier event but also is the only shot with minimal spall. Comparisons between the 6 shots can be seen in Fig. 0-6. [Bowman, 2019] conclude that the acoustic energy radiated from an explosion could be scaled by comparing the logarithm of the energy ratio and the logarithm of SDOB. However, this ratio is currently not a useful metric for investigating underground detonations given the current sparse data available.

[Pasyanos and Kim, 2019] investigated both seismic and acoustic signal characteristics of SPE in comparison with Forensics Surface Explosions (FSE) which are a series of surface explosions [Kim, 2019]. An important observation from the comparison of SPE to FSE can be seen in Fig. 0-7 where a clear difference in behavior between surface and buried explosions is shown. While FSE showed impulsive acoustic signals due to explosive gas expansion and shock generation from

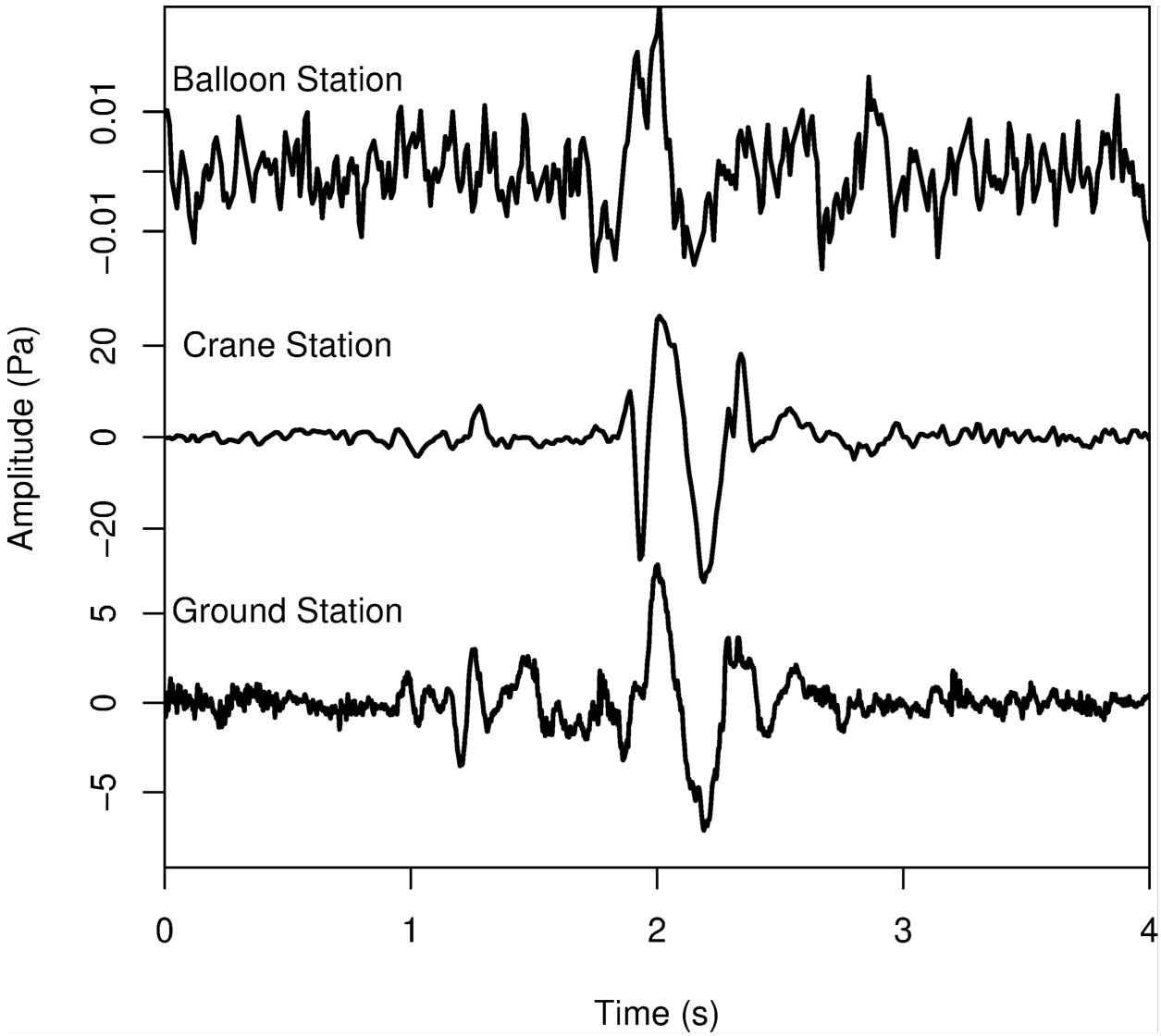

Figure 0-4. A comparison of waveforms recorded on the ground, on the crane, and on the balloon during DAG-4.

surface explosions, SPE signals exhibited relative long duration of pressure disturbances. As discussed previously, this is due to the nature of ground motion (spall) generating acoustic pressure changes in the atmosphere. [Pasyanos and Kim, 2019] estimated both explosion yield and depth-of-burial (DOB)/height-of-burst (HOB) by using seismoacoustic energy partitioning of chemical explosions. It is well known that simultaneous estimation of explosion yield and DOB can be greatly improved by including both seismic and acoustic analysis [Ford et al., 2014]. They further improved the empirical relationship of seismoacoustic energy partitioning depending on depths by including SPE data. Fig. 0-8 shows acoustic impulses, or the source characteristic representing the strength of the acoustic source, observed from SPE Phase I in comparison to the empirical model developed by [Ford et al., 2014]. Ford's empirical models (black lines) were developed by near-surface chemical explosions and significantly underestimated acoustic energies from buried explosions of SPE. By including the SPE observations, [Pasyanos and Kim, 2019]

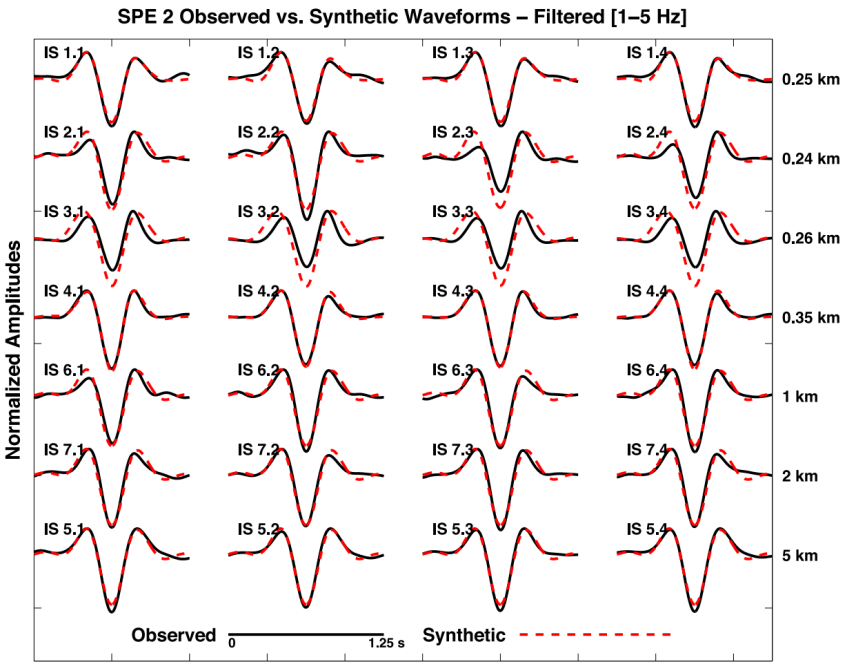

Figure 0-5. Example of the comparison between observed and synthetic waveforms for SPE-2, figure modified from [Jones et al., 2014]

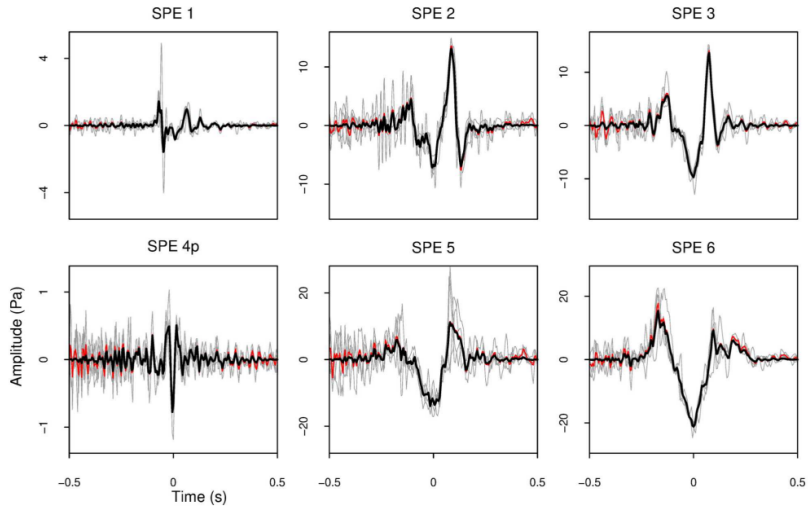

Figure 0-6. Visualization of time traces from IS3 during all of the SPE phase 1 events, where each panel corresponds to one of the SPE events. The gray lines are traces from each of array's sensors aligned on to the maximum rarefaction. The red line is the average value and the black line is the average value with a cosine taper. Notice the odd behavior of SPE-4'. Figure modified from [Bowman, 2019]

improved an empirical acoustic model and extended the seismoacoustic yield estimation for buried explosions. This study also suggested ways in which this methodology could be improved moving forward. The first of these is the suggestion that seismic stations could investigate smaller events by looking at higher frequencies (this study used 2-8 Hz). However, this brings about its

own complications due to the lack of knowledge regarding propagation properties at these high frequencies. The second is that further numerical simulation should be done to improve the relationships developed for the yield and DOB, which field experiments did not cover. While this study investigates the short-range usage of seismoacoustic coupled data, the authors suggest that it can be applicable to regional infrasound propagation if the atmospheric conditions are taken into account.

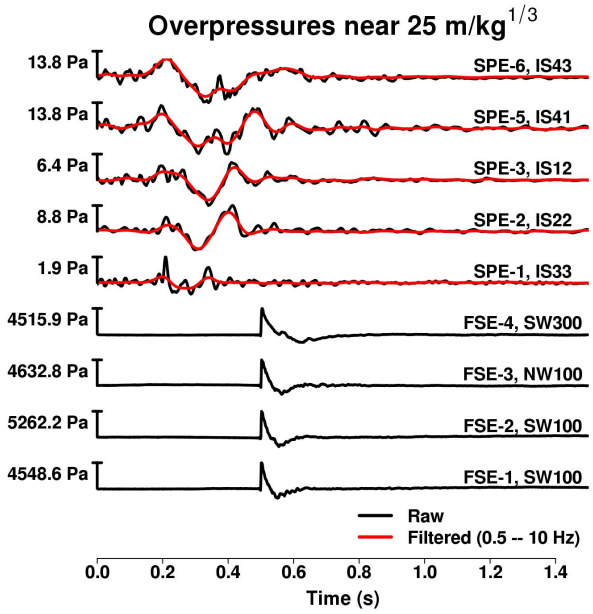

Figure 0-7. Comparison between SPE and FSE events. Showing the dramatic difference between under- ground (SPE) and surface (FSE) explosions. Figure adopted from [Pasyanos and Kim, 2019].

A set of two papers that build off of each other are [Poppeliers et al., 2018] and [Poppeliers et al., 2020]. These papers focus on how the sensitivity of atmospheric conditions contribute to the results of infrasonic inversion. The first focuses solely on the use and development of atmospheric models, known as predictive models, to analyze the sensitivity of the atmospheric conditions on the estimated source properties. These predictive models use only historic and regionally scaled data corresponding to the approximate time of day and day of year for the SPE events. An example of the output from one of the atmospheric models can be seen in Fig. 0-9. The results of this study [Poppeliers et al., 2018] demonstrate that within the range of the experiment (5 km) at the NNSS, small changes in the atmospheric models had no significant impact on the estimated seismoacoustic source function. The primary focus for the follow-up study was to investigate and compare the results of predictive models and postdictive models by including *in situ* high resolution model data or actual measurements made at the time and place of the SPE experiments. The results of [Poppeliers et al., 2020] indicate that the estimated waveform shape is similar no matter what atmospheric model is used to invert the data. The authors do report that predictions carry across the shot series; however, these discrepancies could still be within the uncertainty of the measurements. Finally, authors note that the inclusion of true weather sonde data had negligent effects on the estimated source terms and the "fit-to-date" was very good no matter the model used. It is also important to note that [Poppeliers et al., 2018]

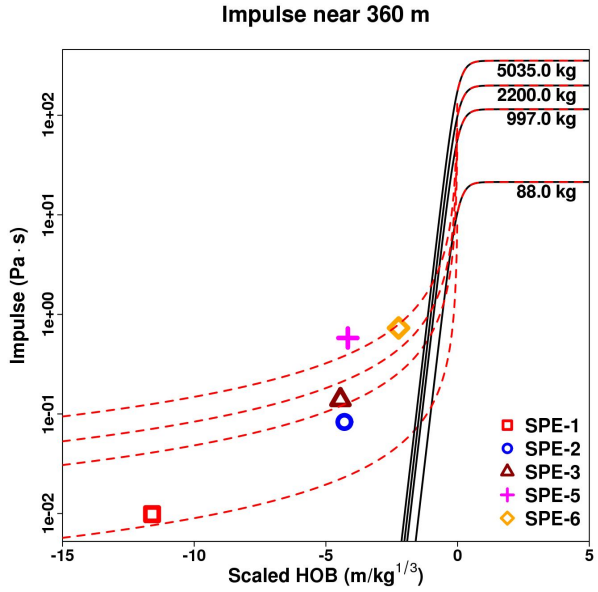

Figure 0-8. Acoustic impulse observation vs. empirical models. SPE data are not fit to the Ford's model (black line) [Ford et al., 2014] which were developed for near-surface explosions. New models (red) are suggested by [Pasyanos and Kim, 2019] by including the SPE observations. Figure is adapted from [Pasyanos and Kim, 2019].

concluded that a source can be represented as single point source at the surface ground zero location.

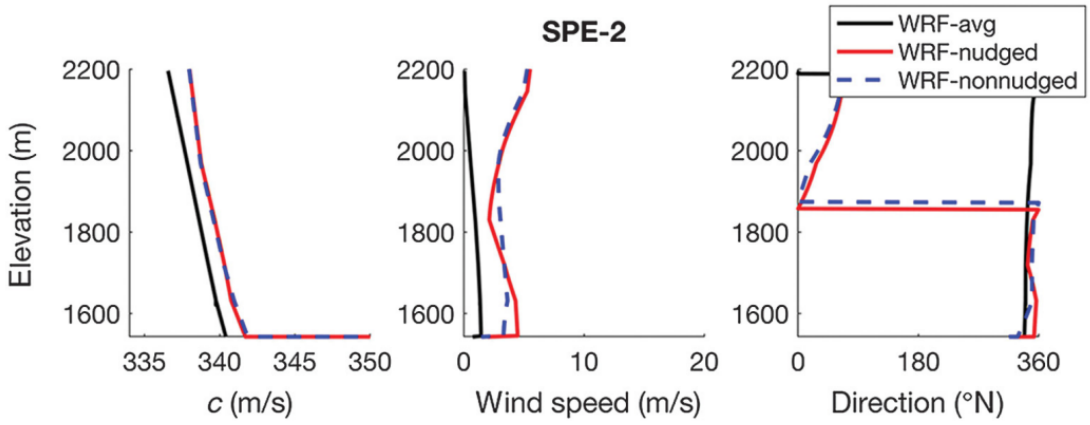

Figure 0-9. A comparison of speed of sound (left), wind speed (middle), and wind direction (right) used for infrasound inversion, figure modified from [Poppeliers et al., 2020]. WRF-avg (black) is based on the predictive method from [Poppeliers et al., 2018] while WRF-nudged (red) utilizes radiosonde data and WRF-nonnudged (blue) does not.

[Blom et al., 2020] extended the ideas presented in [Jones et al., 2014] to construct a

seismoacoustic model through the combination of the Rayleigh integral and a parameterized spall ground motion model. The results of this model agree with those from [Jones et al., 2014], finding that the spall effect is a primary driver for acoustic production. The extended model suggests that if there is no ground failure (i.e., no spall), then only very shallow events will produce horizontally propagating acoustic signals. For events that produce spall, a direct relationship is found between the spall mechanics and signal frequency content such that the frequency content of the horizontally propagating acoustic signal is strongly correlated with the dwell time. The model constructed by [Blom et al., 2020] also provides some explanation for the lack of signal detection in several SPE Phase I and II tests as shown in Fig. 0-10. The spall dynamics (left panel of the figure) define a radius at which the spall closure originates and depth-yield combinations can be identified for which this radius goes to zero. For SPE events shallower than this limiting depth, acoustic signals are typically observed, but for those events near or below the depth (SPE-1 and -4' as well as DAG-1, -2, and -3), little to no acoustic signals are observed. This idealized model is useful to limit possible depths of an explosion with unknown emplacement. However, it is important to note that this study assumed that explosion occurred under a flat surface, meaning that analysis of more events is required for more general application.

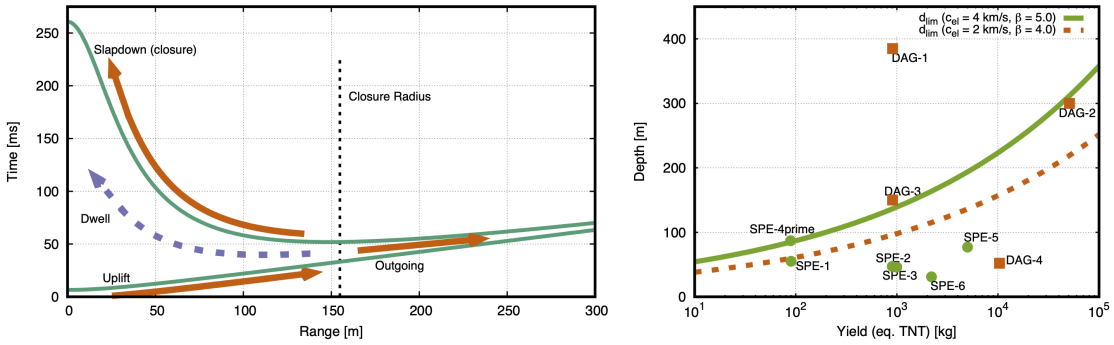

Figure 0-10. Ground motion during spall (left) includes a closure radius at which the slapdown/closure originates. The limiting depth (right) can be identified as that for which the closure radius goes to zero and those SPE and DAG explosions shallower than this depth are found to produce notable acoustic signals. Figures modified from [Blom et al., 2020].

The Rayleigh integral showed great promise to predict infrasound generated by ground motions caused by the SPE tests. However, the derived model is only valid for homogeneous atmospheres over flat surface due to assumptions made during its derivation. This simplification allowed for solving the equation by analytic or relatively simple numerical methods, but it is difficult to apply it to general cases with heterogeneous atmospheres and complex topography. In order to avoid the limitation of the Rayleigh integral, [Kim et al., 2022] introduced distributed point sources for infrasound generation and validated their method by the SPE dataset. The distributed point sources were derived from the Rayleigh integral to represent air volume changes due to the ground motions. For infrasound generation, the series of point sources are equivalent to corresponding ground motions. By incorporating the distributed point source into a finite-difference method, they demonstrated that the point sources converge to the Rayleigh integral for a homogeneous atmosphere with flat surface. The distributed point sources, however, can be used with other numerical methods (i.e., finite-difference) to include complex topography

and atmospheric conditions. Fig. 0-11 shows the results of finite-difference modeling for SPE-6. Distributed point sources equivalent to epicentral ground motions were implemented over local topography. The vertical directionality of infrasound wavefield was affected by the slope of local ground surface. This distributed point source approach does not require flat surface or homogeneous atmosphere conditions and can be used for infrasound generation by any ground motions in realistic scenarios (e.g., earthquakes, landslides).

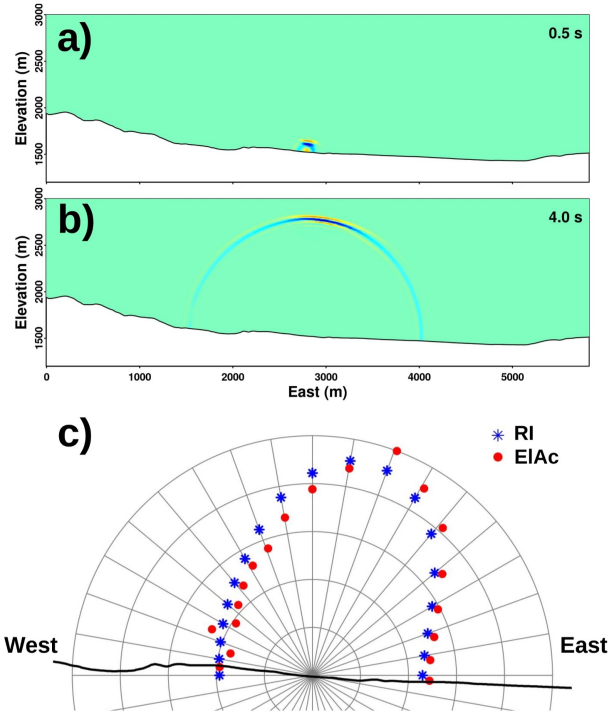

Figure 0-11. Infrasound propagation simulated by a finite-difference code, ElAc, with distributed point sources for SPE-6. ElAc simulation images are plotted for 0.5 s (a) and 4.0 s (b) of elapsed time. Local surface topography is included in the simulation. c) Vertical infrasound amplitude comparison between the finite-difference method (ElAc) and Rayleigh integral (RI). The directionality of infrasound wavefield is affected by local topography. This figure is adopted from [Kim et al., 2022].

[Berg and Poppeliers, 2022] performed a linear inversion of acoustic time-series data to resolve the source parameters of the fourth buried chemical explosion in the DAG series. The estimated source parameters consisted of a combination of direct elastic-to-acoustic coupling at the air-earth interface and ground upheaval, or spall, at the Earth's surface. To estimate these sources, the authors used a three-dimensional, fully coupled, elastic-to-acoustic forward model to predict the recorded acoustic wavefield. Surface acceleration near the buried chemical explosion is predicted to test the ability to constrain the buried source. Synthetic results appears similar to observed vertical accelerometer data. The authors predict infrasound data from both the predicted and observed surface accelerations through the Rayleigh integral. They found that using the predicted surface acceleration in the Rayleigh integral results in simulated infrasound signals that are overamplified compared to observed data, which highlights the limitations of this method. The main findings from this study are that at the local scale, purely linear models can predict the infrasonic signal, but the primary contribution to infrasonic signal is the spall source.

0.4. Conclusions and Experimental Impact

The recently completed Phase I and II series of the Source Physics Experiment provide a wealth of well-constrained seismoacoustic data recorded from 10 distinct underground chemical explosions. The explosions were conducted in two contrasting lithologies, granite and dry alluvium and across a wide range of yields and depths. The overall goal of the SPE program is to improve U.S. nuclear explosion monitoring capabilities, particularly focused on event identification and explosion yield estimation. Initial seismoacoustic research utilizing this dataset has improved source modeling efforts for global monitoring, improving confidence for monitoring future nuclear tests in new areas and emplacements. Results from the research program indicate that:

- Acoustic data from underground explosions can provide constraints on event depth and spall generation mechanisms.
- Spall generates acoustic signals; these in turn can constrain spall models.
- Acoustic signals associated with explosive events such as explosions or shallow earthquakes are generated by a combination of ground motion and topographic effects.
- Source yield and depth-of-burial can be constrained through acoustic energy partitioning of chemical explosions.
- Varying source depths from the SPE series demonstrate an empirical relationship for seismoacoustic energy partitioning as a function of depth.
- A depth-based understanding of acoustic signal generation limits possible depths of future explosions with unknown emplacements.
- A explosive seismoacoustic source can be represented as single point source at the surface.
- At local scales, infrasonic signals can be predicted by purely linear models.

The abundance of high fidelity data from dense networks offers new opportunities within the seismoacoustic community to build upon research efforts highlighted above. Data from the series is available at the Incorporated Research Institutions of Seismology for community use.

Data and code availability

SPE waveform data and metadata were compiled, archived, and distributed by the technical members of the Nevada Seismological Laboratory (NSL) at UNR. Records for stations at greater distances are available from the permanent UNR seismic network. The full data sets for all six SPE tests and all four DAG tests, along with associated metadata, are available from the Incorporated Research Institutions for Seismology (IRIS) Data Management Center. Technical reports accompany each data release with further details on test characteristics and instrumentation.

REFERENCES

[Anderson et al., 2018] Anderson, J. F., Johnson, J. B., Bowman, D. C., and Ronan, T. J. (2018). The gem infrasound logger and custom-built instrumentation. *Seismological Research Letters*, 89(1):153–164.

[ANSI, 1983] ANSI (1983). Estimating air blast characteristics for single point explosions in air, with a guide to evaluation of atmospheric propagation and effects.

[Arrowsmith et al., 2010] Arrowsmith, S. J., Johnson, J. B., Drob, D. P., and Hedlin, M. A. (2010). The seismoacoustic wavefield: A new paradigm in studying geophysical phenomena. *Reviews of Geophysics*, 48(4).

[Berg and Poppeliers, 2022] Berg, E. M. and Poppeliers, C. (2022). Inversion of infrasound time series for seismoacoustic source parameters produced by a buried chemical explosion at the Source Physics Experiment Phase II: Dry Alluvium Geology. *Bulletin of the Seismological Society of America*, pages 1–15.

[Blom, 2020] Blom, P. (2020). The influence of irregular terrain on infrasonic propagation in the troposphere. *The Journal of the Acoustical Society of America*, 148(4):1984–1997.

[Blom et al., 2020] Blom, P., Iezzi, A., and Euler, G. (2020). Seismoacoustic analysis of underground explosions using the Rayleigh integral. *Geophysical Journal International*, 223(2):1069–1085.

[Bowman, 2019] Bowman, D. C. (2019). Yield and emplacement depth effects on acoustic signals from buried explosions in hard rock. *Bulletin of the Seismological Society of America*, 109(3):944–958.

[Bowman and Krishnamoorthy, 2021] Bowman, D. C. and Krishnamoorthy, S. (2021). Infrasound from a buried chemical explosion recorded on a balloon in the lower stratosphere. *Geophysical Research Letters*, 48(21):e2021GL094861.

[Bowman et al., 2020] Bowman, D. C., Norman, P. E., Pauken, M. T., Albert, S. A., Dexheimer, D., Yang, X., Krishnamoorthy, S., Komjathy, A., and Cutts, J. A. (2020). Multihour stratospheric flights with the heliotrope solar hot-air balloon. *Journal of Atmospheric and Oceanic Technology*, 37(6):1051–1066.

[Bowman et al., 2014] Bowman, D. C., Taddeucci, J., Kim, K., Anderson, J. F., Lees, J. M., Graettinger, A. H., Sonder, I., and Valentine, G. A. (2014). The acoustic signatures of ground acceleration, gas expansion, and spall fallback in experimental volcanic explosions. *Geophysical Research Letters*, 41:1916–1922.

[Ford et al., 2014] Ford, S. R., Rodgers, A. J., Xu, H., Templeton, D. C., Harben, P., Foxall, W., and Reinke, R. E. (2014). Partitioning of seismoacoustic energy and estimation of yield and height-of-burst/depth-of-burial for near-surface explosions. *Bulletin of the Seismological Society of America*, 104(2):608–623.

[Hart, 2007] Hart, D. M. (2007). Evaluation of Inter-Mountain Labs infrasound sensors: July 2007. Technical report, Sandia National Laboratories (SNL), Albuquerque, NM, and Livermore, CA.

[Jones et al., 2014] Jones, K. R., Whitaker, R. W., and Arrowsmith, S. J. (2014). Modelling infrasound signal generation from two underground explosions at the Source Physics Experiment using the Rayleigh integral. *Geophysical Journal International*, 200(2):779–790.

[Kim, 2019] Kim, K. (2019). Acoustic source parameters and yield estimation for SPE Phase I and Forensics Surface Events.

[Kim et al., 2022] Kim, K., Bowman, D. C., and Fee, D. (2022). Finite-difference simulation for infrasound generated by finite-extent ground motions. *Seismological Research Letters*.

[Kim and Rodgers, 2017] Kim, K. and Rodgers, A. (2017). Influence of low-altitude meteorological conditions on local infrasound propagation investigated by 3-D full-waveform modeling. *Geophysical Journal International*, 210(2):1252–1263.

[Kinney and Graham, 2013] Kinney, G. F. and Graham, K. J. (2013). *Explosive shocks in air*. Springer Science & Business Media.

[Larotonda and Townsend, 2021] Larotonda, J. M. and Townsend, M. J. (2021). Data release report for the Source Physics Experiment Phase II: Dry Alluvium Geology experiments (DAG-1 through DAG-4), Nevada National Security Site. Technical report, Nevada National Security Site (NNSS), North Las Vegas, NV (United States).

[Pasyanos and Kim, 2019] Pasyanos, M. E. and Kim, K. (2019). Seismoacoustic analysis of chemical explosions at the Nevada National Security Site. *Journal of Geophysical Research: Solid Earth*, 124(1):908–924.

[Patton, 1990] Patton, H. J. (1990). Characterization of spall from observed strong ground motions on Pahute Mesa. *Bulletin of the Seismological Society of America*, 80(5):1326–1345.

[Poppeliers et al., 2018] Poppeliers, C., Aur, K. A., and Preston, L. (2018). The relative importance of assumed infrasound source terms and effects of atmospheric models on the linear inversion of infrasound time series at the Source Physics Experiment. *Bulletin of the Seismological Society of America*, 109(1):463–475.

[Poppeliers et al., 2020] Poppeliers, C., Wheeler, L. B., and Preston, L. (2020). The effects of atmospheric models on the estimation of infrasonic source functions at the Source Physics Experiment. *Bulletin of the Seismological Society of America*, 110(3):998–1010.

[Schnurr et al., 2020] Schnurr, J., Kim, K., Garces, M. A., and Rodgers, A. (2020). Improved parametric models for explosion pressure signals derived from large datasets. *Seismological Research Letters*, 91(3):1752–1762.

[Simmons et al., 2003] Simmons, D., Glenn, L., and Carney, T. (2003). Review of ground shock calculations in hard rock. *Hard Rock Database Review (final report)*.

[Šindelářová et al., 2021] Šindelářová, T., Carlo, M. D., Czanik, C., Ghica, D., Kozubek, M., Podolská, K., Baše, J., Chum, J., and Mitterbauer, U. (2021). Infrasound signature of the post-tropical storm Ophelia at the Central and Eastern European Infrasound Network. *Journal of Atmospheric and Solar-Terrestrial Physics*, 217:105603.

[Snelson et al., 2013] Snelson, C. M., Abbott, R. E., Broome, S. T., Mellors, R. J., Patton, H. J., Sussman, A. J., Townsend, M. J., and Walter, W. R. (2013). Chemical explosion experiments to improve nuclear test monitoring. *Eos, Transactions American Geophysical Union*, 94(27):237–239.

[Snelson et al., 2011] Snelson, C. M., Barker, D. L., White, R. L., Emmitt, R. F., Townsend, M. J., Graves, T. E., Becker, S. A., Teel, M. G., and Lee, P. (2011). The Nevada National Security Site—Source Physics Experiment (SPE-N): An overview. *Proc. of the 2011 Monitoring Research Review: Ground-Based Nuclear Explosion Monitoring Technologies*, pages 578–581.

[Townsend and Mercadente, 2014] Townsend, M. and Mercadente, J. (2014). Data release report for Source Physics Experiment 1 (SPE-1), Nevada National Security Site. Technical report, Nevada Test Site (NTS), Mercury, NV (United States).

[Townsend and Obi, 2015] Townsend, M. and Obi, C. (2015). Data release report for Source Physics Experiments 2 and 3 (SPE-2 and SPE-3) Nevada National Security Site. Technical report, Nevada Test Site/National Security Technologies, LLC., Las Vegas, NV.

[Townsend and Obi, 2017] Townsend, M. and Obi, C. (2017). Data release report for Source Physics Experiment 4Prime (SPE-4Prime) Nevada National Security Site. Technical report, Nevada National Security Site/National Security Technologies, LLC (United States).

[Townsend et al., 2019] Townsend, M., Obi, C., Abbott, R., Bowman, D., Mellors, R., Wharton, S., Schalk, W., Smith, K., Plank, G., Steedman, D., et al. (2019). Data release report Source Physics Experiments 5 and 6 (SPE-5 and SPE-6), Nevada National Security Site. Technical report, Nevada National Security Site (NNSS), Mercury, NV (United States).

[Werth and Herbst, 1963] Werth, G. C. and Herbst, R. F. (1963). Comparison of amplitudes of seismic waves from nuclear explosions in four mediums. *Journal of Geophysical Research*, 68(5):1463–1475.

DISTRIBUTION

Email—Internal

Name	Org.	Sandia Email Address
Technical Library	1911	sanddocs@sandia.gov

Sandia National Laboratories

Sandia National Laboratories is a multimission laboratory managed and operated by National Technology & Engineering Solutions of Sandia LLC, a wholly owned subsidiary of Honeywell International Inc., for the U.S. Department of Energy's National Nuclear Security Administration under contract DE-NA0003525.